2012 IEEE/RSJ International Conference on
Intelligent Robots and Systems
October 7-12, 2012. Vilamoura, Algarve, Portugal

Soft Tactile Sensor Arrays for Micromanipulation

Frank L. Hammond III, *Member, IEEE,* Rebecca K. Kramer, Qian Wan, Robert D. Howe, *Fellow, IEEE*¸ and Robert J. Wood, *Member, IEEE*

***Abstract*—Micromanipulation methods used for complicated tasks such as microrobot assembly and microvascular surgery often lack the force reflection and contact localization capability necessary to achieve robust grasps of micro-scale objects without applying excessive forces. This absence of haptic feedback is especially prohibitive in cases where visual evidence of force application, such as object surface deformation, is imperceptible and where unstructured, dynamically changing environments require force sensing and modulation for safe, atraumatic object manipulation.**

This paper describes the design, fabrication, and experimental validation of a soft tactile sensor array for sub-millimeter contact localization and contact force measurement during micromanipulation. The geometry and placement of conductive liquid embedded channels within the sensor array are optimized to provide adequate sensitivity for representative micro-manipulation tasks. Mechanical testing of the sensor demonstrates a sensitivity of less than 50mN and contact localization resolution on the order of 100's of microns.

I. Introduction

MICROMANIPULATON is an essential capability in many advanced medical procedures and manufacturing processes. Dexterous handling of small, delicate structures such as microparts, surgical needles, and soft, compliant biological tissues requires precise sensing and modulation of manipulation forces in order to prevent unintended damage. However, due to the magnitude of tool-object interaction forces (5-50 mN) and the length of the instruments used during manual micromanipulation, force and tactile information - which are widely regarded as essential for effective object manipulation - are very difficult, if not impossible, to perceive [1-4].

In certain micromanipulation tasks, one can compensate for the absence of direct haptic feedback by using visual cues, such as the changes in material reflectance or shading on the surface of soft, deformable objects (biological tissues), to estimate applied forces [5], or by precisely structuring the manipulation workspace such that object locations and orientations are known a priori (automated pick-and-place assembly tasks). In other cases where workspaces are unstructured, visual acuity is poor, and objects are rigid and do not deform under expected manipulation forces, the lack of haptic feedback can significantly reduce the speed and accuracy of manipulation and, in some instances, render conventional micro-manipulation methods unsafe or intractable. This is especially true in microsurgery, where excessive force application can easily damage surgical tools and lead to iatrogenic tissue trauma [6-8].

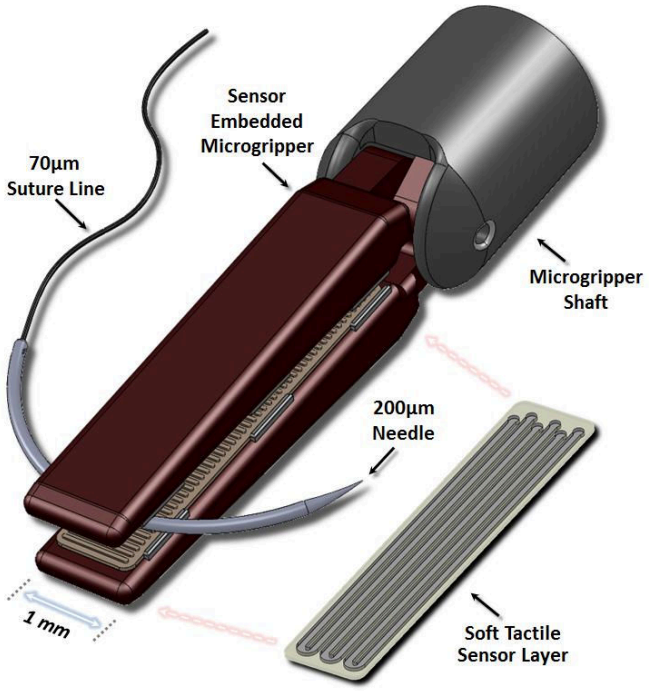

Fig. 1. Conceptual illustration of a surgical microgripper with embedded soft tactile sensor arrays grasping a suturing needle. Embedded sensors could be used to prevent excessive contact forces that could damage delicate needles, biological tissues, and microparts.

Several research efforts have been made in recent years to address the need for haptic feedback in micromanipulation. Piezoresistive strain gauges [9-12] and optical Fiber Bragg Grating (FBG) sensors [13] have been used to measure tool-tip forces, with millinewtons of resolution, in microsurgery devices. Piezoelectric polyvinylidine-floride (PVDF) films [14] and MEMS-based capacitive sensor arrays [15,16] have been used in a variety of robotic micromanipulation applications as tactile sensors. The development of several MEMS-based force sensing micromanipulators for use in microassembly has also been reported [17,18]. Each of these sensing approaches provides precise, repeatable force

Manuscript received March 12, 2012, final paper submitted on July 21, 2012. F. L. Hammond III is with the Harvard School of Engineering and Applied Sciences, 60 Oxford Street, Cambridge, MA 02138 USA (email: fhammond@seas.harvard.edu).

R. K. Kramer, Q. Wan, R. D. Howe and R. J. Wood are with the Harvard School of Engineering and Applied Sciences, 60 Oxford Street, Cambridge, MA 02138 USA (e-mail: rkramer@fas.harvard.edu, {qwan, howe, rjwood} @seas.harvard.edu).

measurement or contact localization suitable for a range micro-manipulation tasks. However, many of them also pose problems with complexity and cost of fabrication, signal processing and temporal hysteresis, packaging and assembly limitations, and a lack of functional versatility (task-specificity) that make them unfit for general-purpose micromanipulation.

Recent advances in flexible electronics have availed a new group of soft, elastic, skin-like sensors that stand to improve the functionality and tractability of force and tactile sensing in general micromanipulation. These flexible sensor technologies range from stretchable conductors [19] and single-walled carbon nanotubes to conductive particle and liquid microchannel embedded elastomers [20-22]. Elastomer-based sensors, due to their ability to undergo and sense high strains, can easily conform to various object shapes. This compliance innately reduces peak pressures and forces [23], improves grasp stability by increasing contact friction, and mitigates the consequences of excessive force application, visual occlusion, or object-microgripper misalignment during grasp acquisition, making conductive liquid embedded elastomer sensors a prime candidate for use as a haptics modality in micromanipulation.

In this study, we design and experimentally validate a soft, conductive liquid embedded tactile sensor array for micromanipulation. This work leverages theory and fabrication methods from recent research on the design of an elastic wearable tactile keypad [24] and on multi-modal, elastomer-based strain sensors [25] to create a soft tactile sensor array with sub-millimeter resolution. The design of this tactile sensor is numerically simulated to ensure adequate sensitivity to the forces and pressures associated with representative manipulation tasks in microsurgery. Through experimental testing, we demonstrate the ability both to measure the relative magnitude of pressures and forces applied to the sensor surface and to estimate the location of the applied force on the sensor array. Such thin, compliant tactile sensors will have applications in many areas of micromanipulation, including the enablement of force feedback in manual tools for microsurgery and assembly, the tactile feedback for dexterous, teleoperative robotic manipulation, and the safe, atraumatic handling of tissues and surgical instruments for the automation of robotic microsurgery tasks (Fig. 1).

II. Sensor Design

The design of the presented soft tactile sensor array is based on the principle that the geometry of a conductive liquid-filled microchannel embedded in an elastic body will change when that body is deformed by compression or stretching, changing its electrical resistance. Assuming that the cross-sectional area of a rectangular microchannel and the electrical properties of the conductive liquid are known, the change in the electrical resistance of the microchannel after deformation due to uniform contact pressure is

$$\Delta R = \frac{\rho L}{wh}\left\{\frac{1}{1-2(1-\nu^2)wp/Eh}-1\right\} \quad (1)$$

where ΔR is change in resistance, ρ is electrical resistivity, L is microchannel length, w and h are the width and height of the microchannel cross-section, p is a uniform contact pressure and ν and E are the Poisson's ratio and elastic modulus of the elastic material, respectively [25] (Fig. 2). If modeled properly, conductive liquid microchannel geometries can be tuned such that their total range of electrical resistance spans the range of expected pressures or forces that deform the channels, thus providing sufficient sensitivity for a given set of tasks.

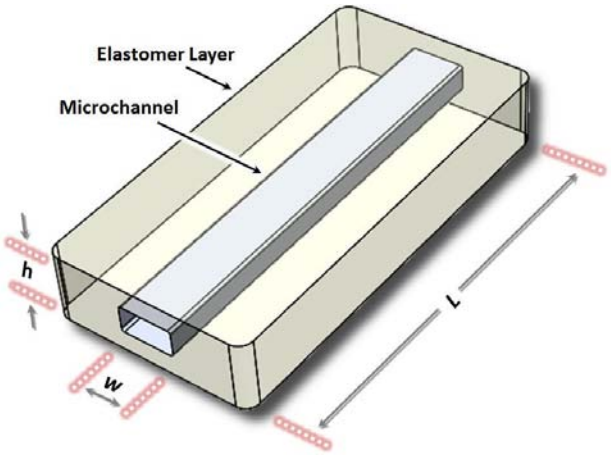

Fig. 2. Concept drawing of a conductive liquid filled microchannel embedded in an elastomer layer. Major dimensions used to compute microchannel resistance are shown.

A. Target Application and Performance Requirements

The soft tactile sensor presented here is designed for use in dexterous microsurgery procedures. The performance requirements for this tactile sensor, drawn from demanding microsurgery tasks including retinal microsurgery [11,13] and small blood vessel anastomosis, are as follows:

- *Force and Pressure Sensitivity*: Microsurgical force characterization experiments [26] posit that the maximum force seen in micromanipulation is approximately 1.0N. Setting a minimum sensing resolution of 1/10th the maximum expected force and assuming that force can be distributed across up to four tactile pixels (taxels) at once, each sensor taxel must be sensitive enough to respond to 25mN of force.
- *Spatial Resolution and Taxel Size*: Each sensor taxel must be small enough to fit across the contact pads of standard manual microsurgery forceps and localize contact along the smallest dimension (~1mm wide). Microchannel width is set to 400μm to provide contact localization (2 taxels) along the width of the forceps surface, with 200μm of space for channel walls/septum.

- *Overall Tactile Array Size*: Manual microsurgery forceps tips generally have a width of ~1mm and height of 1-2mm. Assuming a thickness of 1mm from the contact surface to the back side of each forceps jaw, we posit that half of this height can be used for sensor housing, making the maximum sensor height 500µm.

These performance requirements serve as the basis both for the design space constraints employed during numerical simulation of microchannel deformation and for the experimental methods used to characterize the functional range and sensitivity of the soft tactile sensor.

B. Tactile Sensor Topology

The soft tactile sensor benchtop prototype is comprised of two layers of microchannel-embedded polydimethylsiloxane (PDMS), arranged in an orthogonal configuration. By using one channel-embedded layer to sense contact in each direction in the plane, a two-dimensional matrix of taxels is created (Fig. 3). Much like the sensing elements on modern touch-screens, these taxels can be used for contact localization and pressure measurement. The proposed tactile sensor contains eight taxels in a 2x4 configuration.

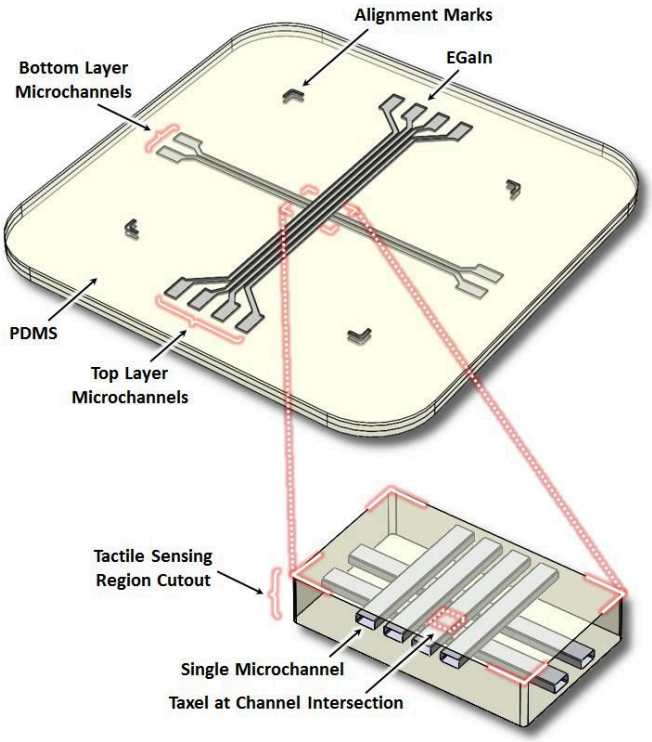

Fig. 3. The soft tactile sensor morphology with orthogonal microchannels for contact localization; the primary sensor region is highlighted.

The degree of microchannel deformation under a given load and, by extension, the overall sensitivity of the elastic sensor, is governed by microchannel geometry, elastomer material properties, and the position of the embedded channel within the elastomer. Recent work [22] derived an analytical approximation to model changes in microchannel cross-section with respect to these variables. However, this analytical solution is not appropriate for cases where microchannels are relatively large with respect to the dimensions of the elastomer, as they are in this tactile sensor. Here, the microchannels are close both to the elastomer surface and in proximity to each other for higher sensitivity and spatial resolution. To design tactile sensors that are sensitive enough for micromanipulation, we first model and simulate the non-linear elastic mechanics using finite element analysis (FEA).

C. Microchannel Design Simulation

Simulation of the tactile sensor microchannel geometry was done in COMSOL 4.1a Multiphysics software (COMSOL, Inc., Burlington, Massachusetts, USA). A single microchannel was modeled parametrically by height h_{chan}, width w_{chan}, and channel depth h_{depth} (Fig. 4). To capture the non-linear elastic behavior of the PDMS under large strain, the FEA simulation was set up as a stationary solid mechanics problem with a Mooney-Rivlin hyperelastic material model. PDMS material properties were set to the following values: density ρ = 965 kg/m^3, Young's modulus E = 500kPa, Poisson's ratio ν = 0.5, shear modulus G = 250kPa, and Mooney-Rivlin parameters C_{10} = 75.5kPa and C_{01} = 5.7kPa [27].

The microchannel-embedded PDMS layer model was given a fixed motion constraint on its bottom boundary and a pressure field on its top boundary corresponding to a given force distributed over four sensor taxels. A uniform pressure load, which varied with changes in cross-sectional area, was applied to the internal boundary of the microchannel. Pressure changes induced within the microchannel by the displacement of conductive liquid (incompressible) were roughly approximated using the expression shown in (2).

$$\Delta P_{int\_rel} = \eta \cdot P_{atm}\left(\frac{A_{init}}{A_{new}} - 1\right) \quad (2)$$

Here, P_{int_rel} is the relative internal pressure of the microchannel assuming the external pressure is constant, A_{init} is the initial microchannel cross-sectional area, A_{new} is the cross-sectional area of the deformed microchannel, P_{atm} is the atmospheric pressure, and η is the expansion factor (set to 0.2) which accounts for the pressure relieved when a channel expands due to conductive liquid displacement.

The optimization of the microchannel geometry to meet performance requirements was accomplished by varying the channel height and surface thickness parameters, and by comparing cross-sectional area changes over the force range of 25-250mN, distributed evenly as a pressure over 1.0mm^2 - the area covered by four taxels. Microchannel width w_{chan} was held constant at 400 µm to meet aforementioned sensor size requirements. Both the microchannel height h_{chan} and the contact surface thickness h_{surf} were varied from 20µm to 200µm in increments of 20µm. The total sensor thickness t_{sensor} was limited to a maximum of 500µm, with the remaining material serving as the microchannel substrate.

Due to variations in the material stiffness and shape of objects (biological tissues, surgical instruments), we expect the proposed tactile sensor to experience both distributed and point loads during micromanipulation. To ensure adequate sensitivity for either loading case, we based our FEA simulations on distributed loads as they would likely cause less microchannel deformation for a given force, and thus induce a weaker sensor response, than a point load.

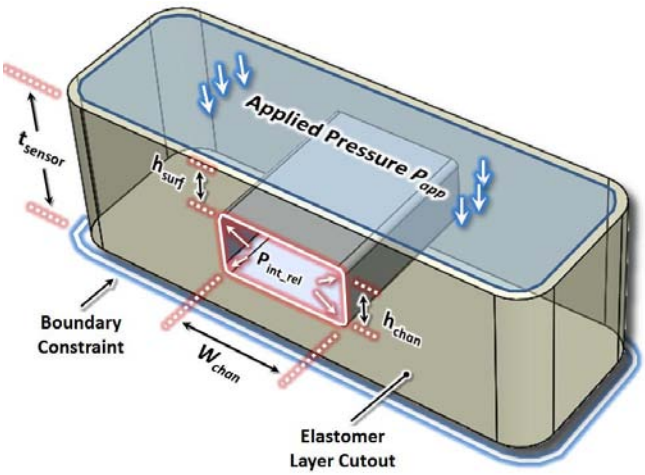

Fig. 4. Illustration of the design parameters used in simulating and optimizing the soft tactile sensor microchannel geometry. Pressure is applied to the top surface of the sensor, while a fixed boundary constraint is applied to the bottom surface. A reactive internal pressure is applied to the channel surface as the microchannel deforms.

D. Results of Single Channel Optimization

The numerical search of the microchannel design space yielded a set of sensor designs which, by FEA simulation, seem suited to sensing the target micromanipulation forces (as low as 25 mN). Microchannel geometries with very thin surface layers, 20-80µm, were the most sensitive channels, but also involved the largest strains and lowest ranges of sensitivity. Microchannel geometries with greater height, 100-160µm, and embedded under more than 100µm were generally too insensitive to the 25mN minimum forces, with resistance changes as low as 3.6%. The most suitable performance came from microchannel designs with 20-60µm heights and 100-160µm surface layers (Fig. 5). These microchannel geometries exhibited adequate resistance changes and ranges of sensitivity for the specified performance requirements, and resulted in form factors thin enough allow for two sensing layers - under 500µm in total thickness – necessary for 2D contact localization.

E. Extension to Multi-layer Sensor Design

An additional FEA simulation was conducted to estimate the amount of sensitivity achievable by stacking two sensing layers, orthogonally as in Fig. 3, to form the 2x4 taxel tactile sensor. This two-layer sensor was modeled and simulated using the same material properties and boundary conditions prescribed for the previous simulations. The sensor design parameters were chosen based upon results from the microchannel simulation experiment. The tactile sensor microchannels were modeled with a height of 20µm, with surface layers 140µm thick. A 100µm-thick layer of PDMS was used as the sensor base.

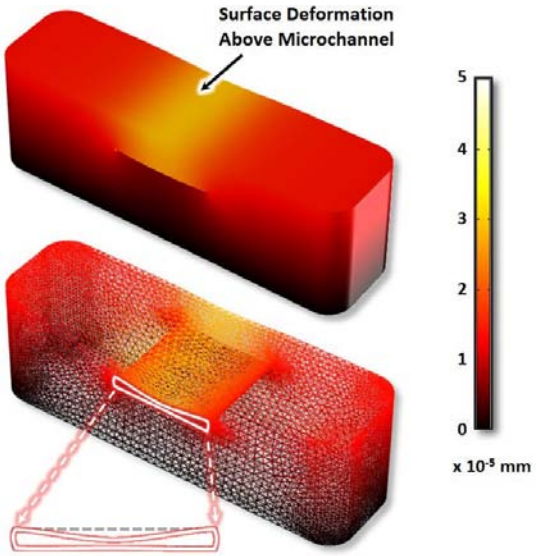

Fig. 5. COMSOL simulations of a microchannel, with a 140µm surface and a 20µm height, under a distributed pressure load. Unlike other microchannel geometries, this type of geometry (low height, thick surface layer) is very sensitive to pressure for less significant surface deformation.

Results of the tactile sensor simulation (Fig. 6) suggest that microchannel sensitivity is adequate in both range and magnitude. The applied pressure caused a 69.5% micro-channel cross-sectional area decrease on the top sensor layer, corresponding to a 228% increase in resistance, and a 38.2% decrease in the bottom layer channels, corresponding to a 62% increase in resistance – both changes are measurable using standard data acquisition equipment.

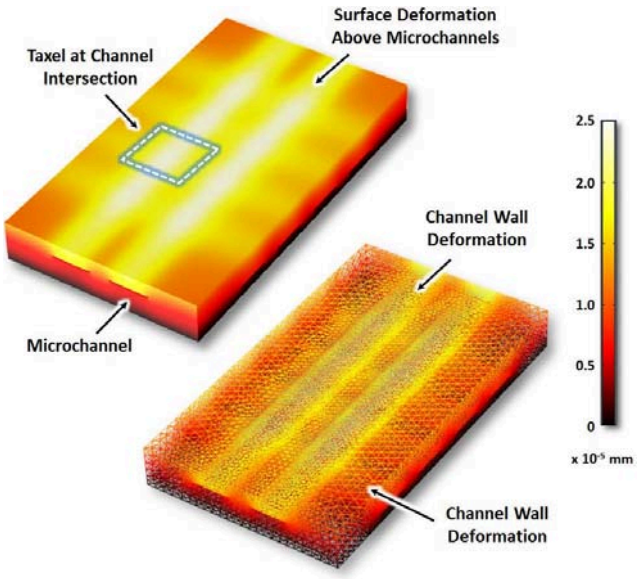

Fig. 6. Results of the full soft tactile sensor FEA simulation. Surface plot shows deformations on sensor surface due to microchannel collapse under distributed load. The wireframe plot shows channel wall deformations.

III. Fabrication

After using the simulation results to inform the soft tactile sensor design, a sensor array was fabricated by means of a soft lithography process (see [24] for process illustration). Photoresist (SU-8 2010) was spun onto a clean silicon wafer to achieve a film thickness of 20µm. After a soft-bake, the coated wafer was then patterned by use of a photomask followed by a hard-bake and developer step. Silicon masters are used to mold three PDMS layers that result in the sensor array. A hydrophobic monolayer was introduced by vapor deposition to discourage adhesion between the silicon molds and subsequently cured PDMS. The wafers were placed in an evacuated chamber (20 mTorr) with an open vessel containing a few drops of Trichloro (1H,1H,2H,2H-perfluorooctyl) silane (Aldrich) for 3 hours.

PDMS (Sylgard 184, Dow Corning) was spin-coated in liquid form (10:1 weight ratio of elastomer base to curing agent) onto a silicon mold to result in a thin elastomer film of tunable thickness. Each PDMS layer was cross-linked by heat-curing at 60°C for 30-40 minutes. Layers were manually removed from the molds and bonded together via oxygen plasma surface treatment, conducted at 65 Watts for 30 seconds. In order to accommodate subsequent filling of the channels within such a thin device using conventional syringe dispensing, small blocks (~1cm^2) of PDMS were adhered to each channel inlet and outlet location using uncured elastomer as adhesive glue. Introducing small holes into the adhered inlet and outlet blocks provided a convenient method for manual injection of the conductive liquid eutectic Gallium Indium (eGaIn). External wiring was achieved by manually cutting off the inlet/outlet block, inserting copper wire into the channel ends, and sealing the channels with a droplet of uncured PDMS. The final device thickness was approximately 350µm (Fig. 7).

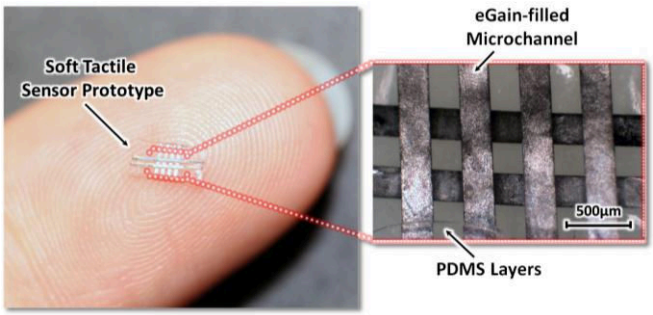

Fig. 7. The soft tactile sensor prototype fabricated for experimentation.

IV. Experimental Validation

The soft tactile sensor experimental setup is comprised of commercial data acquisition hardware and electromechanical testing equipment. The prototyped tactile sensor was empirically characterized by applying various forces to the sensor at several taxel locations using a custom designed tactile sensor testbed and recording corresponding changes in the electrical resistances of the microchannels.

A. Mechanical Testing Setup

The soft tactile sensors were tested using an electro-Instron 5540 Series mechanical testing system and the soft tactile sensor testbed (Fig. 8). The Instron load frame was equipped with a 10N load cell capable of ±0.5% reading accuracy down to 1/250 (40mN) of cell capacity. The custom designed tactile sensor testbed (Fig. 9), rapid-prototyped using the Objet Connex500^{TM} 3D printer (Objet Inc.), consisted of a base plate for placement and alignment of the tactile sensor, and a force application plate with interchangeable micro-patterned contact pads (Fig. 10). Guide posts on the base plate hold the force application plate in alignment with the sensors. The Instron system was used to characterize the stiffness of the springs before sensor testing to remove the spring force bias from measurements.

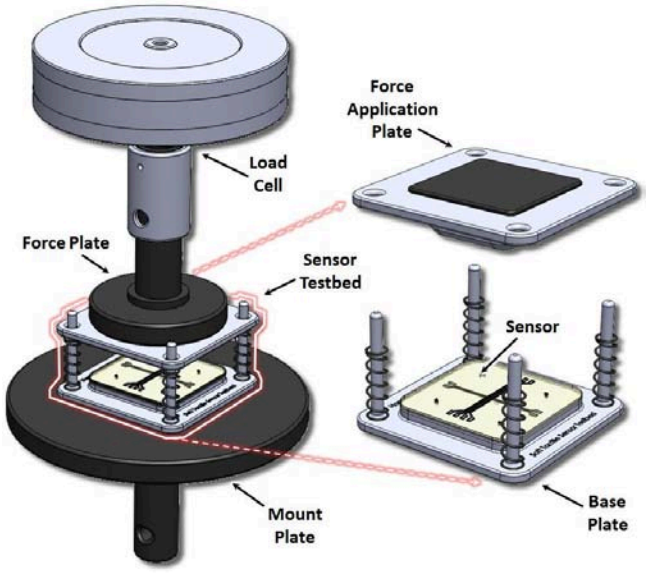

Fig. 8. Soft tactile sensor mechanical testing setup, with Instron 5540 Series electromechanical testing system and custom designed sensor testbed.

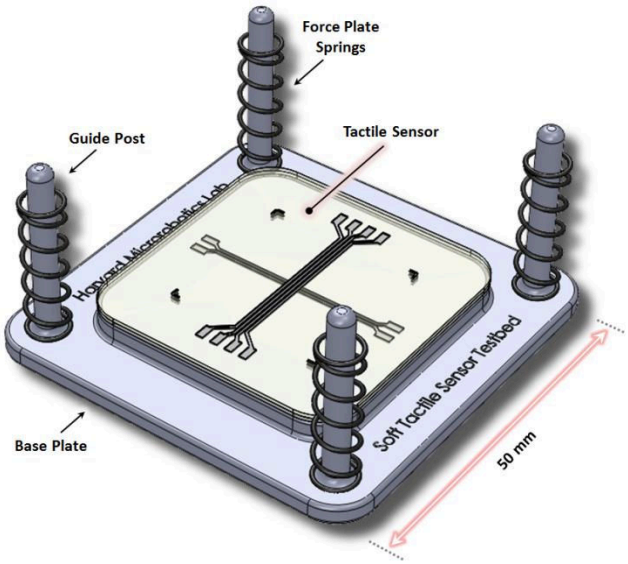

Fig. 9. Components of the rapid-prototyped soft tactile sensor testbed baseplate, with tactile sensor mounted.

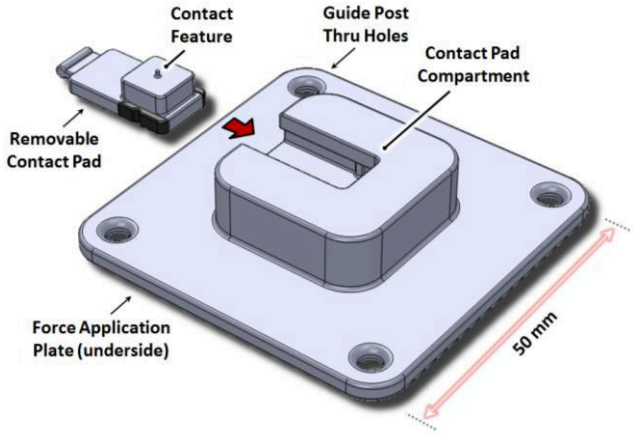

Fig. 10. Components of the soft tactile sensor testbed force application plate (underside) with removable contact pad.

B. Data Acquisition

The ends of the soft tactile sensor eGaIn channels were wired to a National Instruments data acquisition (DAQ) board through a set of voltage divider circuits. Each microchannel was connected to a single divider with a reference resistor R_{ref} of 10Ω and a common power source V_S of 2.0V (Fig. 11). Increases in the electrical resistance R_{chan} of an eGaIn channel, due to external forces, causes an increase in voltage at the divider output node. That voltage output is governed by

$$V_{chan} = \frac{R_{chan}}{R_{ref} + R_{chan}} \cdot V_S \qquad (3)$$

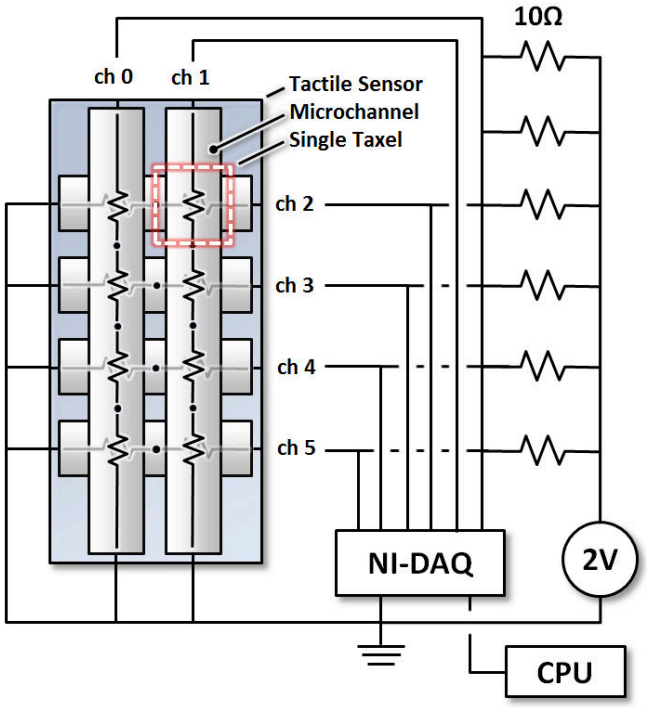

Fig. 11. An electrical schematic of the experimental setup for soft tactile sensor array mechanical testing. Resistances within the microchannels, dictated by the tactile array configuration, are shown.

The voltage divider readings for each channel were acquired by a National Instruments DAQ interface, sampled at 10kHz. Voltages were recorded from all six microchannels during the mechanical testing of the sensor, and the resulting empirical data were used to validate the sensor's force sensitivity and contact localization ability.

C. Mechanical Test Procedure

The fabricated soft tactile sensor was mounted to the sensor testbed base plate and mechanically tested using five different contact pads, shown in Fig. 12. For each contact pad, the Instron load frame applied 0.0mN to 100mN of force to the sensor by slowly pushing the testbed force application plate down at 50µm per second. The voltages across the sensor microchannels were recorded using the NI DAQ system until the load cell reached the set maximum force limit, after which the Instron load frame returned to the initial position. Trials were run for each of the contact pads. The recorded data was used to characterize the sensitivity of the tactile sensor and the ability to localize contact pressure on and across individual sensor taxels.

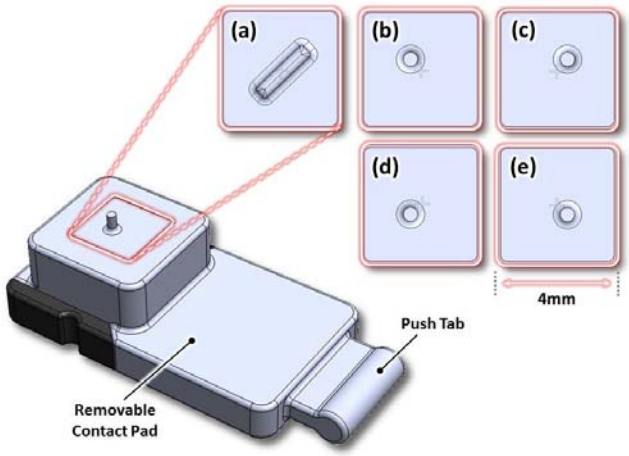

Fig. 12. The contact pads used for mechanical testing the response of the soft tactile sensor: (a) a diagonal bar feature designed to compress all channels at once to test microchannel response within and between layers, (b-e) pads with single 500µm diameter cylindrical indenter features designed to apply loads to one of the four taxels located at the sensor center.

From these tests, three important sensor performance characteristics were analyzed:

- *Microchannel Pressure Sensitivity*: Demonstrated by applying force over one taxel and measuring the response of the top layer microchannel.
- *Contact Localization*: Demonstrated by applying force over one taxel and comparing the response of the target taxel microchannels to the adjacent microchannels.
- *Multi-layer Microchannel Sensitivity*: Demonstrated by applying force over one taxel and measuring the response of both top and bottom microchannel.

V. Results

A. Pressure Sensitivity

The response from the top layer microchannel of the target taxel, loaded by forces applied with the contact pad in Fig. 12.b, indicates a smooth, nearly linear sensitivity to forces under 100mN, with the output voltage increasing by approximately 45% from 0.505V to 0.732V (Fig. 13). This linear response contrasts with the highly nonlinear responses seen in prior work [24]. This is due in large part to the design of the microchannel geometry, which requires little surface deformation to cause large resistance changes. For small deformations of the channel surface, the force-deformation relationship remains in its linear region, thus the changes in channel cross-sectional area due to applied forces tend to exhibit a similar relationship.

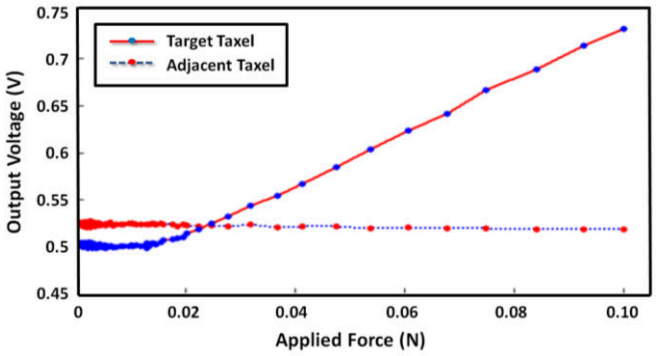

Fig. 13. Sensor outputs versus load applied using the contact pad in Fig. 12-b, and forces applied over sensor channels 0 and 3 (Fig. 11). The Instron system had a force reading bias of ~20mN prior to sensor loading. The initial voltage of ~0.505V corresponds to a target taxel channel resistance of 3.67Ω. The adjacent channel shows a slight decrease in resistance.

B. Contact Localization

The top layer microchannel of a sensor taxel adjacent to the target taxel exhibited only a 1% change in output voltage, indicating its relative insensitivity to contact occurring outside of its contact surface area. This shows that the proposed tactile sensor can be used to accurately localize individual contact points within the sensor's taxel array without significant aliasing.

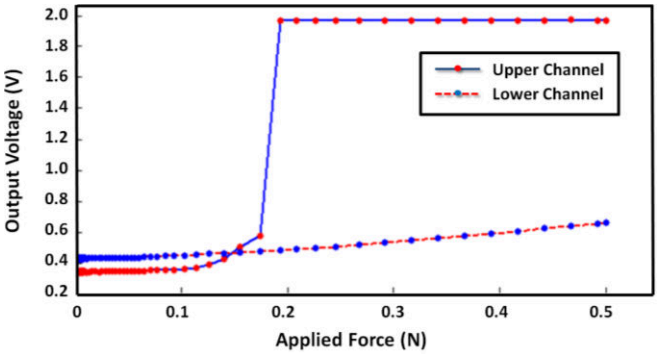

Fig. 14. Sensor output versus load applied using the contact pad in Fig. 11.a, with forces applied over sensor channels 0 and 3 (Fig. 10). The Instron system had a force reading bias of ~5mN prior to sensor loading.

C. Multi-layer Pressure Sensitivity

Applying a point load over one taxel caused deformation of channels in both the top and bottom layers, but the bottom layer, due to additional material between the sensor surface and the microchannel surface, exhibited less sensitivity than the top layer channels. Figure 14 shows the disparity in channel response between the layers, with the bottom layer showing a weaker response to applied force. As the applied force approaches 180mN, the top microchannel collapses completely and saturates the output voltage at 1.97V. The bottom channel saturates much later, at 1008mN of force.

VI. Discussion

The goal of this work was to design, fabricate, and empirically characterize a soft tactile sensor for use in micromanipulation. The results show that our numerical modeling techniques and design considerations, combined with a novel soft sensor fabrication method [24], led to an effective solution for sub-millimeter contact localization and micron-level force sensing. This study has provided several important insights into soft tactile sensor fabrication and illuminated areas for improvement the design methodology.

A. Fabrication Insights

In this work, we noticed a strong correlation between load distribution and sensor sensitivity to contact pressure. This follows intuition, given that distributed load will yield less deformation and the sensors react to elastic deformation. Therefore, we induce that for a point load, elastic deformation is extremely localized and severe. In order to exploit this, sensor array features and densities must correlate to anticipated point load feature lengths, thus introducing a conceptual design method for distinguishing very localized and discrete pressures.

However, due to the increased elastic deformation induced by point loads, microchannels are more susceptible to "pinching", where the channels walls are collapsed by the load and the channel response is saturated. This saturation point is a function of channel aspect ratio (i.e. sensitivity), such that relatively insensitive channels can measure greater applied loads before saturation than can very sensitive channels. During experimentation, we found some intermittent delamination between layers, causing some conductive liquid to flow out of the microchannels and between the layers. While channels still remained functional and conductive, the internal pressure of the channels was likely affected and may have contributed to early sensor saturation during tests. "Over-filling" the microchannels and maintaining a high internal pressure would probably improve the functional range of sensors in future devices.

B. Sensor Design Methodology

The FEA-based design methodology used in this work focused primarily on optimizing microchannel geometries for sensitivity to minimum expected forces. It did not consider, however, designing channels in different layers

with layer-specific aspect ratios that 1) compensate for strain attenuation through varying amounts of surface material and 2) allow for matching resistance changes and saturation points across all microchannels, regardless of the layer. Multi-layer sensitivity experiments revealed large disparities in channel response due to sensitivity mismatches between layers. Future design efforts will address this mismatch problem and will consider improvements to our FEA such as a more rigorous formulation for internal microchannel pressure, and consideration of the changes in tactile sensor performance under combined normal and shear forces.

VII. Conclusion and Future Work

In this paper, a soft tactile sensor was designed sensing in micromanipulation. The tactile sensor was designed to localize contact with sub-millimeter resolution and to sense forces on the order of 10's of mN – meeting the levels of performance required for targeted microsurgical procedures. The tactile sensor microchannel geometry was numerically simulated and tuned in FEA software to fit these performance requirements, and a prototype sensor was fabricated and empirically tested to characterize performance and validate the design. The sensor proved capable of fulfilling both performance requirements.

Future work will focus on 1) refining fabrication methods to produce tactile arrays with higher spatial resolution and smaller scale, 2) the design of multi-modal sensors capable of sensing pressures and normal and shear forces, 3) multi-touch sensor arrays that can better discriminate larger or multiple contact locations during micromanipulation, and 4) sensor aliasing for inter-taxel contact localization.

Acknowledgment

The authors gratefully acknowledge the Wyss Institute for Biologically Inspired Engineering and the National Science Foundation for their support of this work. Any opinions, findings, and conclusions or recommendations expressed in this material are those of the authors and do not necessarily reflect the views of the National Science Foundation. F. L. Hammond III thanks the National Academy of Sciences for financial support through the Ford Foundation Postdoctoral Fellowship Award. R. Kramer thanks the NSF Graduate Fellowship Program for financial support.

References

[1] C. Wagner, N. Stylopoulos, R. Howe, "The Role of Force Feedback in Surgery: Analysis of Blunt Dissection," in *Proc. 10th Symposium on Haptic Interfaces for Virtual Environment and Teleoperator Systems,* Orlando, FL, USA, pp. 68-74, 2002.

[2] G. Tholey, J.P. Desai, and A.E. Castellanos, "Force Feedback Plays a Significant Role in Minimally Invasive Surgery: Results and Analysis," *Annals of Surgery*, vol. 241, no. 1, pp. 102-109, 2005.

[3] C-H. King, et al., "Tactile Feedback Induces Reduces Grasping Force in Robot-Assisted Surgery," *IEEE Transactions on Haptics,* vol. 2, no. 2, pp. 103-111, 2009.

[4] J. Stoll and P. DuPont, "Force Control for Grasping Soft Tissue," *Proc. of IEEE Int. Conf. of Robotics and Automation*, Orlando, FL, 2006, pp. 4309-4311.

[5] A.R. Lanfranco, A.E. Castellanos, J.P. Desai, and W.C. Meyers, "Robotic Surgery - A Current Perspective," *Annals of Surgery*, vol. 239, pp. 14-21, 2004.

[6] S. De et al., "Assessment of Tissue Damage due to Mechanical Stresses," *IEEE/RAS-EMBS Int. Conf. on Biomedical Robotics and Biomechatronics*, Pisa, Italy, 2006. pp. 823-828.

[7] D. Marucci, J. Cartmill, W. Walsh, and C. Martin, "Patterns of Failure at the Instrument-Tissue Interface," *Journal of Surgical Research*, vol. 93, pp. 16-20, 2000.

[8] J. Cartmill, A. Shakeshaft, W. Walsh, and C. Martin, "High Pressures are Generated at the Tip of Laparoscopic Graspers," *Aust. N.Z. Journal of Surgery*, vol. 69, pp. 127-130, 1999.

[9] A. Menciassi et al., "Force Feedback-Based Microinstrument for Measuring Tissue Properties and Pulse on Microsurgery," *IEEE/ASME Trans. on Mechatronics*, vol. 8, no. 1, pp. 10-17, 2003.

[10] K. Houston et al., "Polymer sensorized microgrippers using SMA actuation," in *Proc. IEEE International Conference on Robotics and Automation*, Roma, Italy, 2007.

[11] P. K. Gupta, P. S. Jensen, "Surgical Forces and Tactile Perception During Retinal Microsurgery," *Medical Image Computing and Computer-Assisted Intervention (MICCAI)*, pp. 383-390, 1999.

[12] P. J. Berkelman, L. L. Whitcomb, R. H. Taylor, and P. Jensen, "A miniature microsurgcial instrument tip force sensor for enhanced force feedback during robot-assisted manipulation," *Robotics and Automation, IEEE Trans. on* , vol.19, no.5, pp. 917- 921, Oct. 2003.

[13] Z. Sun et al., "Development and Preliminary Data of Novel Optical Micro-Force Tools for Retinal Surgery," in *Proc. IEEE Int. Conf. on Robotics and Automation*, Kobe, Japan, 2009, pp. 1897-1902.

[14] M. A. Qasaimeh, S. Sokhanvar, J. Dargahi, and M. Kahrizi, "PVDF-Based Microfabricated Tactile Sensor for Minimally Invasive Surgery," *Journal of Microelectromechanical Systems*, vol. 18, no. 1, pp. 195-207, February 2009.

[15] S. Sokhanvar, M. Packirisamy, and J. Dargahi, "A multifunctional PVDF-based tactile sensor for minimally invasive surgery," *Smart Materials and Structures*, vol. 16, pp. 989–998, Aug. 2007.

[16] B.L. Gray, R. S. Fearing, "A surface micromachined microtactile sensor array," *IEEE Int. Conf. of Robotics and Automation*, Minneapolis, MN, USA, 1996.

[17] K. Kim, X. Liu, Y. Zhang, and Y. Sun, "MicroNewton Force-Controlled Manipulation of Biomaterials Using a Monolithic MEMS Microgripper with Two-Axis Force Feedback," in *Proc. IEEE International Conference on Robotics and Automation (ICRA '08)*, Pasedena, CA, USA, 2008, pp. 3100-3105.

[18] H. Chu, J. Mills, and W. Cleghorn,"MEMS Capacitive Force Sensor for Use in Microassembly," in *Proc.of IEEE/ASME Int. Conference on Advanced Intelligent Mechatronics*, Xi'an, China, 2008, pp. 797-802.

[19] Y. Sun, W. Choi, H. Jiang, Y. Huang, and J. Rogers, "Controlled buckling of semiconductor nanoribbons for stretchable electronics," Nature nanotechnology, vol. 1, no. 3, pp. 201–207, 2006.

[20] S. Lacour et al., "Stretchable gold conductors on elastomeric substrates," *Applied physics letters*, vol.82, p. 2404, 2003.

[21] D. Cotton, I. M. Graz, and S. P. Lacour, "A multifunctional capacitive sensor for stretchable electronic skins," *IEEE Sensors Journal*, vol. 9, no. 12, pp. 2008–2009, 2009.

[22] Y. L. Park, C. Majidi, R. Kramer, P. Berard, R. J. Wood, "Hyperelastic Pressure Sensing with a Liquid-Embedded Elastomer," *Journal of Micromechanics and Microengineering*, vol. 20, 2010.

[23] D. Marucci, J. Cartmill, C. Martin, and W. Walsh, "A Compliant Tip Reduces the Peak Pressure Laparoscopic Graspers," *Aust. N.Z. Journal of Surgery*, vol. 27, pp. 476-478, 2002.

[24] R. Kramer, C. Majidi, and R.J. Wood," Wearable Tactile Keypad with Stretchable Artificial Skin," in *Proc. IEEE Int. Conf. on Robotics and* Automation, Shanghai, China, 2011, pp. 1103-1107.

[25] Y. L. Park, B. Chen, R. J. Wood, "Design and Fabrication of Soft Artifical Skin using Embedded Microchannels and Liquid Conductors," *IEEE Sensors Conference*, Limerick, Ireland, 2011.

[26] D-S. Kwon et al., "Microsurgical Telerobot System," *IEEE/RSJ Int. Conf. On Intelligent Robots and Systems*, Victoria, Canada, 1998.

[27] S-H. Yoon, V. Reyes-Oritz, K-H. Kim, Y. Ho Seo, M. R. K. Mofrad, "Analysis of Circular PDMS Microballons With Ultralarge Deflection for MEMS Design," *Journal of Microelectromechanical Sys.*, vol. 19, no. 4, pp. 854-864, 2010.